Proceedings of the
47th IEEE Conference on Decision and Control
Cancun, Mexico, Dec. 9-11, 2008

Linear, Parameter-Varying Wheel Slip Control for Two-Wheeled Vehicles

Matteo Corno, Sergio M. Savaresi and Gary J. Balas

Abstract— **This paper describes the application of Linear Parameter-Varying (LPV) control design techniques to the problem of wheel slip control for two-wheeled vehicles equipped with electromechanical front wheel brakes. A nonlinear multi-body motorcycle simulator is employed to derive a control oriented wheel slip dynamic model. It is shown that, in order to devise a robust and performing controller, it is necessary to take into account the model dependence on velocity and wheel slip. This dependence is modeled via an LPV system and an LPV controller is synthesized. Nonlinear simulations indicate that the proposed controller achieves the needed robustness and performance.**

I. INTRODUCTION

An anti-locking brake system (ABS) controls the slip of the wheels of a vehicle to avoid locking and the consequent loss of friction and steerability [1]. In the past few years, with the introduction of more sophisticated actuators, the goal has shifted from avoiding locking to modulating wheel slip [2], [4].

Two-wheeled vehicles are lacking behind in this developments. This is due to several factors; among the technological causes it should be noted that most anti-lock braking systems employ an additional hydraulic pump and valves to regulate the pressure of the brake calipers [5]. These systems cannot modulate the braking torque in a smooth way and this often results in annoying vibrations. Several interesting works are found addressing this issue ([6], [7]). Most of the previous work is focused on the problem of braking during a straight run. The problem of braking in turn in addressed, to the best of Authors' knowledge, only in [8].

The study of motorcycles dynamics is a more complex task than the one of four-wheeled vehicles. In the past years the complexity involved in modeling and simulation could be tackled thanks to the use of multi-body approach. Many authors have developed simulators [9], [10], [11] and studied motorbike stability under different driving conditions. Multi-body simulators are well suited for dynamic modal analysis, but they are often too complex for model based control system design. Another critical aspect involved in two-wheeled vehicles simulation is road-tire interaction modeling. This topic has been treated, for example, in [12], [14].

The main contribution of this paper is a model based design of a wheel slip controller for a two-wheeled vehicle. We consider straight trajectories and electromechanical actuators in order to avoid the daunting vibrations associated with ABS systems. A multi-body simulator is employed to obtain a family of linear models that describe the slip dynamics for different working conditions, namely longitudinal velocity and wheel slip. The linearized models allow to employ linear, parameter-varying (LPV) techniques to design a wheel slip controller that can smoothly track slip commands. Nonlinear simulations are used to show that the LPV controller exhibits good behavior both in terms of performance and robustness.

The paper is organized as follows: in Section II the multi-body simulator and the linearization of the wheel slip dynamics are described and analyzed. Section III offers a review of the LPV control synthesis and presents a modification of the synthesis algorithm used to solve controller interpolation issues. Section IV is devoted to the design of the LPV controller which is finally validated, in Section V, through nonlinear simulations.

II. THE MOTORCYCLE MODEL

In this Section the LPV model of the front wheel slip under straight braking is derived. The present study is based on the simulator developed by Dinamoto group [11]. The multi-body model takes into account complex phenomena like tire relaxation length, non linear suspension characteristics, tire stiffness, aerodynamics and rider attitude. The road-tire interaction is modeled according to Pacejka's magic formula [12]. Fig. 1 shows the friction curves for the front and rear tires on dry asphalt. Friction curves plot the longitudinal friction coefficient as a function of the longitudinal slip according to the following definitions:

$$\begin{array}{ll} \lambda & = \frac{v-\omega r}{v} \\ F_x(\lambda) & = \mu_x(\lambda) F_z \end{array} \quad (1)$$

where F_x and F_z are, respectively, the longitudinal force exerted by the tire and the vertical load acting on the tire; v is the longitudinal velocity of the vehicle; ω is the wheel angular velocity and r is the rolling radius of the tire. From figure it can be seen that the peak of the front tire characteristic is around a slip value of about 15% while for the rear tire is slightly lower. The present work is focused on the control of the front wheel slip; as shown in [15] the front wheel slip is responsible for most of the braking force.

Reviewing the ABS literature, it can be noted that most model-based controllers for cars are designed using a single wheel model composed of a wheel attached to a mass m; as the wheel rotates a longitudinal force, F_x is generated by the friction between the road and the tire. The longitudinal force

M. Corno and S. M. Savaresi are with Dipartimento di Elettronica e Informazione, Politecnico di Milano, Piazza L. da Vinci, 32, 20133 Milano. ITALY {corno, savaresi}@elet.polimi.it

G. J. Balas is with the Department of Aerospace Engineering, University of Minnesota, Minneapolis, MN 55455, U.S.A.

978-1-4244-3124-3/08/$25.00 ©2008 IEEE

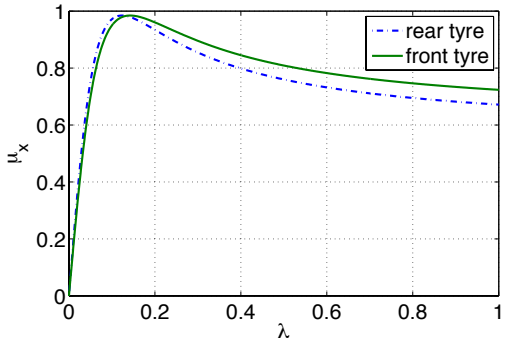

Fig. 1. Front and rear friction curves.

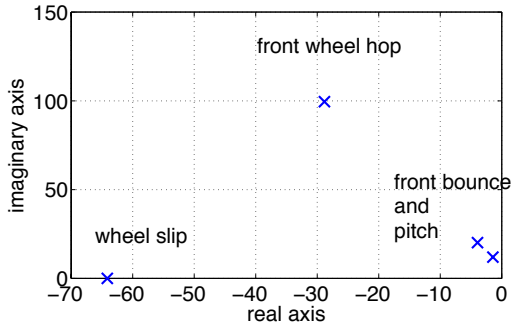

Fig. 2. The 7 most relevant modes of the linearized dynamics.

yields a torque that results in an angular motion of the wheel. The brake actuator generates a braking torque, T_b that slows down the wheel. The equations of motion of single wheel model are:

$$\begin{aligned} m\dot{v} &= -F_x \\ J\dot{\omega} &= rF_x - T_b sign(\omega) \end{aligned} \tag{2}$$

where, beside the symbols already defined, J is the wheel inertia. If the velocity is regarded as a slow time-varying parameter, one can show, by linearization, that the transfer function from braking torque to wheel slip takes the form of:

$$G_\lambda(s) = \frac{r}{Jv} \frac{1}{s + \frac{\mu_1(\bar{\lambda})}{mv}((1-\bar{\lambda}) + \frac{mr^2}{J})} \tag{3}$$

where $\bar{\lambda}$ is the slip around which the dynamic is linearized and $\mu_1(\lambda)$ is the first derivative of $\mu(\lambda)$. The linearized dynamics has one pole whose position mainly depends on the velocity and on the wheel slip. The problem with the single wheel model is that it fails to model load transfer dynamics; this phenomenon can be neglected in four-wheeled vehicles or other vehicles with a long wheelbase compared to the height of the center of mass, but it is of paramount importance for two-wheeled vehicles.

A more complete model can be obtained by Jacobian linearization of the multi-body simulator. The linearization has been executed for different velocities (ranging from 5 to 120 km/h) and slips coefficients (from 0% to 15% - which is at the peak of friction curve). A total of 225 models have been computed. The linearized models have 28 states; when considering only straight trajectories the lateral dynamics is not excited and therefore the states describing those modes are not needed. After reduction, 7 states are maintained; the reduced order model modes are depicted in Fig. 2 and are associated to in-plane vehicle dynamics:

- 1 real pole. It is the wheel slip pole that is captured also by the single wheel model;
- 1 couple of complex poles at a frequency of around 17 Hz which represents the front wheel hop mode;
- 2 couples of complex poles at a frequency of around 2-3 Hz which are associated with the front suspension bounce and motorcycle pitch dynamics.

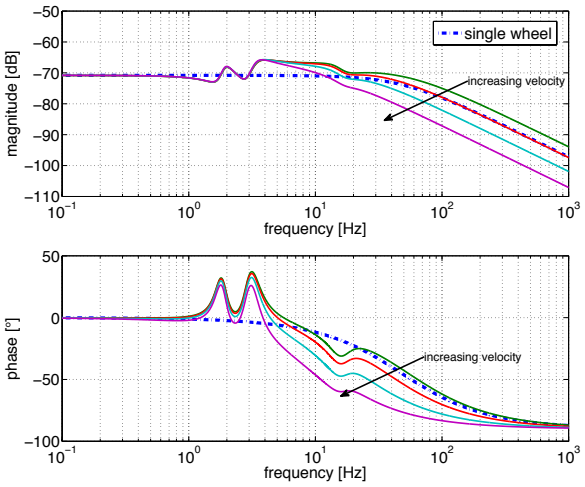

Fig. 3. Bode diagrams of the linearized models as the velocity varies from 15 to 115 km/h.

It is important to point out that the linearized models are not obtained around an actual steady state. In fact, when linearizing around a wheel slip the vehicle is decelerating at a constant deceleration and thus the velocity will vary. The linearized model captures the dynamical behavior of the system up to braking torque steps of around 75 Nm for the case with no initial slip. The linearization neighborhood is much smaller when the initial slip condition is greater than 0; this can be explained by the fact that in this case the velocity drops more rapidly and this will drive the system out of the linearization neighborhood faster.

The set of linearized models allow to study the dynamics dependence on the velocity and wheel slip from a control standpoint; this analysis is aided by Fig. 3 and 4. The first plot depicts the system frequency response as the velocity varies from 15 to 115 km/h for a front wheel slip of 5% the second plots the systems as the slip varies from 0 to 15% while running at 20 km/h. In the linearized models, the wheel slip pole behaves as predicted by the single wheel model. As the velocity decreases the wheel slip pole move toward high frequencies; the same happens if the linearization slip is decreased. The advantage of using the linearized model is the ability to capture load transfer dynamics which are visible as

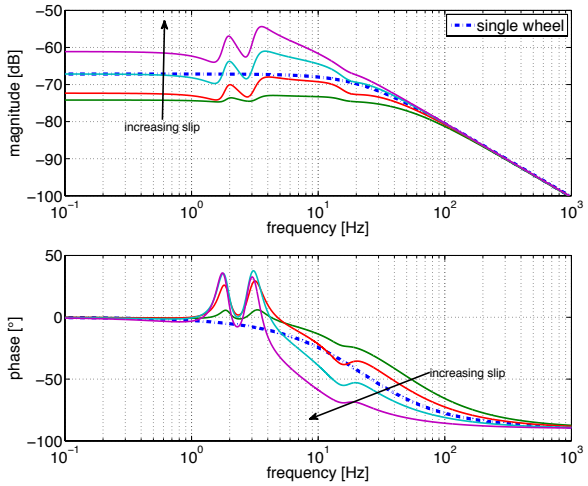

Fig. 4. Bode diagrams of the linearized models as the slip varies from 1% to 15%.

resonances. The importance of load transfer dynamics here is manifest. In Fig. 4, the linearized model for low wheel slip values matches well the first order dynamic described by the single wheel model; but as the slip increases the two models show their differences. Three phenomena are observable:

- the gain of the transfer function increases - this phenomenon is accounted for also by the single wheel model via the first derivative of the friction curve;
- the front wheel slip pole moves toward the imaginary axis;
- the bounce and pitch modes becomes more evident. This is due to the changes in the load distribution. As the deceleration increases, more load is transferred to the front wheel, the front suspension fork compresses and its reduced stiffness varies. This phenomenon is not accounted for by the single wheel model.

Fig. 4 clearly shows the importance of wheel slip and load distribution. As it will be shown, the maximum achievable bandwidth of a wheel slip control system is limited by the actuator delay to [5-20] Hz; not only the greatest spread of phase is around those frequencies, but the vertical dynamics falls around the same frequencies. This makes the ability of taking into account the full model of paramount importance in the design of the controller.

Another important element of the system that needs to be modeled is the brake actuator. In the past few years electromechanical brakes technology has matured to the point where dependable and safe electromechanical brakes are now available. Modern brake-by-wire systems do not rely on a mechanical or hydraulic connection between the brake pedal and the brake itself but they are based on TTP (time-triggered protocol) communication between sensors, ECU and actuators [16]. In this work the brake-by-wire system is considered as a whole and modeled as a first order system with a bandwidth of 12 Hz and pure delay of 5 ms which models the communication protocol and sampling delays. It is clear that the pure delay represents a critical issue when designing the slip controller. A delay of 5 ms in the control loop limits the achievable bandwidth to the range were the system is more sensitive of variation of slip and velocity and where the vertical dynamics is excited.

III. LPV SYSTEMS

The theory of LPV systems has been extensively documented in [17], [18], [19], [20]; in the present Section only the main results useful for the slip controller synthesis will be discussed; attention will be dedicated to present a slight modification of the synthesis algorithm that allowed to solve some controller interpolation smoothness issues. If the open-loop generalized plant is defined as:

$$\begin{bmatrix} \dot{x} \\ e_1 \\ e_2 \\ y \end{bmatrix} = \begin{bmatrix} A(\rho) & B_{11}(\rho) & B_{12}(\rho) & B_2(\rho) \\ C_{11}(\rho) & 0 & 0 & 0 \\ C_{12}(\rho) & 0 & 0 & I_{n_u} \\ C_2(\rho) & 0 & I_{n_y} & 0 \end{bmatrix} \begin{bmatrix} x \\ d_1 \\ d_2 \\ u \end{bmatrix}$$

where $\rho(t)$ is an exogenous variable, belonging to a connected, compact set $\mathcal{P} \in \mathcal{R}^s$ such that $|\dot{\rho}(t)| \leq v$ then the rate-bounded LPV synthesis problem can be stated as:

Theorem 3.1: LPV Control Synthesis
Given a finite number of scalar, continuously differentiable functions $\{f_i\}_{i=1}^N$ and $\{g_i\}_{i=1}^N$ which will be referred to as basis functions, with parametrization

$$X(\rho) = \sum_{i=1}^{N} f_i(\rho) X_i, \quad Y(\rho) = \sum_{i=1}^{N} g_i(\rho) Y_i.$$

There exists a controller which pass the closed-loop stability test if there exist matrices $\{X_i\}_{i=1}^N$, $X_i \in S^{n\times n}$ and $\{Y_i\}_{i=1}^N$, $Y_i \in S^{n\times n}$ such that for all $\rho(t) \in \mathcal{P}$

$$X(\rho) > 0, \tag{4}$$
$$Y(\rho) > 0, \tag{5}$$
$$\begin{bmatrix} X(\rho) & I_n \\ I_n & Y(\rho) \end{bmatrix}, \tag{8}$$

(6) and (7), where - omitting the ρ dependency -

$$\hat{A} = A - B_2 C_{12}, \quad B_1 = \begin{bmatrix} B_{11} & B_{12} \end{bmatrix},$$
$$\tilde{A} = A - B_{12} C_2, \quad C_1^T = \begin{bmatrix} C_{11}^T & C_{12}^T \end{bmatrix}.$$

Once the functions $X(\rho)$ and $Y(\rho)$ are found, the admissible controller state space realization can be computed simply by plugging the two functions in the equations reported in [18]. The synthesis equations are not reported; suffice to note that they have a direct dependence on the open-loop system. The synthesis conditions consist of $2^{s+1}+1$ LMI's which must hold for all $\rho(t) \in \mathcal{P}$. It is still an infinite dimension problem; in order to solve this convex problem the common procedure is based on parameter space gridding. By gridding the parameter space, the synthesis equations will provide a set of LPV controllers which guarantees local stability and performance near the grid points used in the design. Outside the grid vertexes, these controllers are linearly interpolated based on the nearest vertexes. In this setting a trade off arises: if a hyper-rectangle $\mathcal{P} \in \mathcal{R}^s$ is

$$\begin{bmatrix} \sum_{i=1}^{N} f_i(\rho)\left(X_i\hat{A}^T(\rho)+\hat{A}^T(\rho)X_i\right)-\sum_{j=1}\pm\left(v_j\sum_{i=1}^{N}\frac{\partial f_i}{\partial\rho_j}X_i\right)-B_2(\rho)B_2^T(\rho) & \sum_{i=1}^{N} f_i(\rho)X_iC_{11}^T(\rho) & B_1(\rho) \\ C_{11}(\rho)\sum_{i=1}^{N} f_i(\rho)X_i & -I_{n_{e_1}} & 0 \\ B_1(\rho) & 0 & -I_{n_d} \end{bmatrix} < 0 \quad (6)$$

$$\begin{bmatrix} \sum_{i=1}^{N} g_i(\rho)\left(Y_i\tilde{A}^T(\rho)+\tilde{A}^T(\rho)Y_i\right)-\sum_{j=1}\pm\left(v_j\sum_{i=1}^{N}\frac{\partial g_i}{\partial\rho_j}Y_i\right)-B_2(\rho)B_2^T(\rho) & \sum_{i=1}^{N} f_i(\rho)X_iB_{11}^T(\rho) & C_1(\rho) \\ B_{11}^T(\rho)\sum_{i=1}^{N} g_i(\rho)Y_i & -I_{n_{e_1}} & 0 \\ C_1(\rho) & 0 & -I_{n_d} \end{bmatrix} < 0 \quad (7)$$

gridded with L points in each dimension, then the convex problem requires the solution of $L^s(2^{s+1}+1)$ LMI's. On one hand the complexity of the feasibility problem grows as the resolution of the grid to the power of the parameter space dimension; on the other hand a tight grid guarantees a better description of the system and a smoother interpolation. It has been Author's experience that the controller interpolation may pose a problem if the grid is too loose. In order to solve this problem a double grid synthesis is proposed. The proposed synthesis method, based on two grids (a first, looser grid referred to as grid A, and the second finer grid, Grid B), is outlined in the following:

1) The LMI's described by conditions (4-8) are solved on Grid A and the weights of the basis functions $\{f_i\}_{i=1}^N$ and $\{g_i\}_{i=1}^N$ found.
2) The basis functions are evaluated on grid B. $X(\rho_k)=\sum_{i=1}^N f_i(\rho_k)X_i$, $Y(\rho_k)=\sum_{i=1}^N g_i(\rho_k)Y_i$ where ρ_k are the vertexes of Grid B.
3) The open loop system is *re-sampled* on Grid B, finding $A(\rho_k)$, $B(\rho_k)$, $C(\rho_k)$, $D(\rho_k)$.
4) The matrices $A(\rho_k)$, $B(\rho_k)$, $C(\rho_k)$, $D(\rho_k)$ and $X(\rho_k)$, $Y(\rho_k)$ are used to synthesize the controller on Grid B according to the cited equations found in [18].

It is clear that the proposed method does not address the curse of dimensionality involved in the rate-bounded synthesis problem, nevertheless it is found to improve the interpolation phase of synthesis. It allows to increase controller smoothness without increasing the complexity of the problem.

Another problem affecting the synthesis of LPV controllers is the presence of high frequency modes in the controller; in the present synthesis this issue has been solved with the scheme proposed in [17], which uses the solution of the standard LPV problem as the starting point to compute a second solution with additional constraints on the poles.

IV. WHEEL SLIP CONTROL SYNTHESIS

This Section describes the design of a slip controller for the motorbike modeled in Section II. The goal is controlling the slip of the front wheel avoiding the uneasy chattering usually associated with classical ABS. Analyzing Fig. 3 and 4 it is clear that a fixed controller cannot provide both performance and robustness under all conditions. The pure delay in the loop limits the maximum achievable bandwidth to about 10Hz, a range of frequencies where the system is very sensitive to variation of slip and velocity. In order to guarantee stability the controller must be designed on the worst case, namely the one with the greatest phase loss; by doing so one necessary limits the performance in other cases.

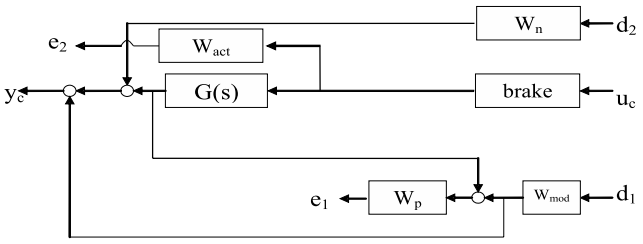

Fig. 5. Wheel slip control system interconnections.

The problem can be solved by making the controller adapt to the plant dynamics; this can be achieved through the LPV framework. Fig. 5 depicts the interconnections diagram used to define the design objectives. In particular, the selected weighting functions are:

1) The control problem is formulated as a model matching problem. $W_{mod}(s)$ represents the second order model to be matched. An natural frequency of 9 Hz and damping coefficient of 0.9 are chosen so to guarantees a well damped response with a settling time of about 0.1s.

2) The error between the desired response and the actual response is the weight $W_p(s)$ which is chosen as a first order low pass filter with a pole in 4 0.001; this ensures very little or no DC error.

3) An output disturbance model is included in the interconnection to increase robustness of the closed loop system. In the synthesis, the weight function is kept constant over all frequencies thus modeling white measurement noise.

4) W_{act} allows to account for bound on the control action. the following actuator weight is used

$$W_{act}(s)=\mu\frac{1/0.001s+1}{1/300s+1}.$$

It allows to penalize use of the actuation above 10 Hz. The gain of the weight function is chosen so that the peak braking torque required to track step requests of slip up to 10% does not exceed 1200 Nm.

5) The electromechanical-brake is modeled as a first order low pass filter and a 2nd order Padé approximation of a 5 ms delay.

6) $G(s)$ models the single input - single output, slip dynamics adjusted with a scaling and normalizing factor. Two scheduling parameters have been taken into account, slip (λ) and velocity (v).

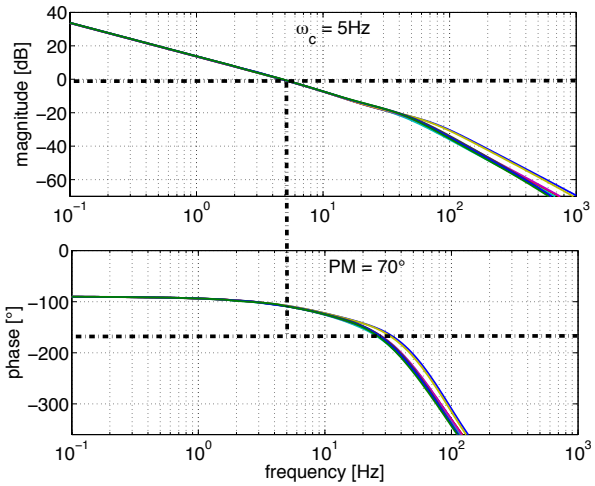

Fig. 6. Controlled plant open loop transfer functions.

As already pointed out the LPV control synthesis is computationally intense so particular care was put in treating this aspect; following the double grid method proposed, two LPV systems are created. The first is created on the same, high density, linear grid described in Section II; the second grid is built on a looser grid where the wheel slip dimension is linearly spaced while a logarithmic spacing is used for the second parameter. The reason for this choice is to be searched in the transfer function (3). It shows that the slip dynamics is more sensitive to velocity variation at low speed. The basis functions used to approximate the infinite dimensional LPV problem are:

$$\begin{aligned} X(v,\lambda) &= X_0 + vX_1 + \lambda X_2 \\ Y(v,\lambda) &= Y_0 + vY_1 + \lambda Y_2 \end{aligned}$$

The induced $\mathcal{L}_2$ norm is 1.41 and the synthesis took 3542 CPUs. The resulting scheduled controller has order 14. Fig. 6 shows the linear analysis of the open loop transfer functions at the grid vertexes; the Bode diagrams show that the performance and stability are guaranteed point-wise with a bandwidth of 5Hz and a phase margin of 70 meaning that the design goals are successfully met in the linear domain.

V. SIMULATION RESULTS

In the previous Section, it was shown that the LPV controller achieves good closed-loop performance for the LPV system. This section is devoted to test the LPV controller on the complete nonlinear multi-body motorbike simulator. The performance in the nominal case and robustness against different road and motorcycle conditions are assessed. Fig. 7 depicts the closed-loop response to a slip reference step in different conditions. On the left hand plot the response to a small (3%) step is depicted; the right hand plot shows the results of a more realistic test. In the latter case a step of 10%

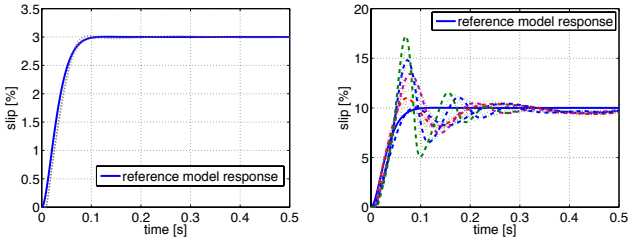

Fig. 7. Nonlinear closed-loop step responses. Small decelerations (left), emergency braking (right).

of slip is requested to simulate a realistic emergency braking. Each plot shows different responses ranging from 120 km/h to 5 km/h. Studying the results for small step around a null slip, it is clear that the linear approximation is valid. More interesting conclusions can be drawn form the 10% response:

(1) the reference model is not perfectly matched. Slip overshoot up to 16% can be observed. These overshoots are similar to the ones seen in slip controllers for four-wheeled vehicles [2]; it is important to note that the bigger overshoot happens at slow speed. The 16% overshoot happens at 10 km/h: as already explained controlling the slip at low speed is very difficult and common ABS systems are simply shut down below a velocity threshold. As already pointed out the degradation is due to the difficulties associated with obtaining a linear model for high slip conditions. Model linearized around high slip conditions have a smaller validity neighborhood and therefore the interpolation introduces more errors than around small slip conditions. This fact introduces a trade off in designing the grid.

(2) The responses exhibit an oscillatory behavior. Oscillations are however damped in less that 0.4 s and are not believed to be felt by the rider as uneasy.

(3) As it can be seen in Fig. 9, the torque applied by the front brake is well within the limit of an electromechanical brake. The peak torque is around 450 Nm, less than a half of what a common electromechanical brake can exert.

The LPV controller has been designed on a grid that does not include slip values above the peak. While this, theoretically, is a limitation - because the single wheel model is unstable for values above the peak - it does not impede the controller robustness. This is true for two reasons: firstly, the slip dynamics can be easily stabilized as it is clear from (3) and, secondly, there is no reason to willingly work in those conditions. For each slip value above the peak there is a correspondent value below the peak that guarantees the same braking force. For these reasons, it is important to guarantee that the controller can safely handle over-the-peak slips but fine control in those condition is of no practical interest. The stability of the controller for over-the-peak condition is partially shown in Fig. 7: the slip overshoot at 10 km/h clearly surpasses the limit and the controller does not lose stability. A more complete simulation study of this condition can be found in the left hand plot of Fig. 8. The figure shows two step responses for two different velocities.

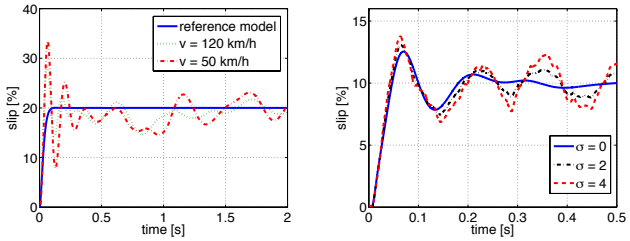

Fig. 8. Nonlinear closed-loop step responses. Over-the-peak target slip (left), noisy measurements (right).

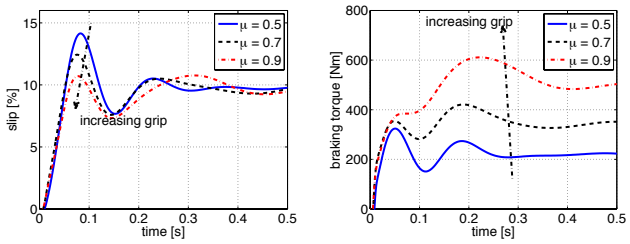

Fig. 9. Nonlinear closed-loop step responses for different road conditions. wheel slip (left) braking torque (right).

Although the performance is greatly degraded the controller can achieve the required slip. The performance suffers from such a degradation because the requested slip is outside the grid used to design the controller. One could enlarge the grid but this, given the computational complexity, would require a looser grid and therefore yield worse performance in the slip region of interest. The right hand plot of Fig. 8 depicts the effect of a noisy slip measurement (note that, to improve readability, the figure depicts the real slip, not the measured one which is fed into the controller), wheel slip measurement and estimation is out of scope of this work; thus a white noise has been assumed: as it can be appreciated by the figure the controller is robust against high level of noise. Note that a noise with $\sigma = 4$ yields a greater noise than a very crude estimation based on front and rear wheel velocity difference.

Finally the controller is tested with different road conditions. Most road surfaces can be modeled as a linear scaling of the friction curve; three road conditions are assumed: the nominal road condition, a slippery surface and a high grip surface). The results can be appreciated in Fig. 9. A firm tire-road grip guarantees a better damping in the response. Surfaces which offer a better grip require higher braking torques to achieve the same slip. For the target slip condition in analysis, the motorbike is subjected to a deceleration of 0.85, 0.6 and 0.4 g respectively for the high grip, nominal and slippery road.

VI. CONCLUSIONS AND FUTURE WORKS

In the present work, the problem of designing a wheel slip controller for motorbikes under straight running conditions has been addressed in a theoretical and simulation-based study. A multi-body nonlinear simulator has been employed to obtain an LPV model of the front wheel slip dynamics; the vehicle longitudinal velocity and instantaneous front wheel slip are treated as exogenous parameters. The problem was addressed by designing an LPV slip controller scheduled on the two exogenous parameters. An approximation scheme useful to improve the smoothness of LPV controller was presented. Nonlinear simulations show that the devised controller guarantees good performance and robustness under different conditions. These results seem to indicate that the approach is promising and currently the real time implementation of the LPV controller is under investigation.

REFERENCES

[1] SAE, "Antilock Brake Review," Society of Automotive Engineers, Warrendale, PA, Tech. Rep.

[2] T. Johansen, J. Petersen, J. Kalkkuhl, and J. Ldemann, "Gain-scheduled wheel slip control in automotive brake systems," *IEEE Transactions on Control Systems Technology*, vol. 11, no. 6, pp. 799–811, November 2003.

[3] S. Solyom, A. Rantzer, and J. Ludermann, "Synthesis of a Model-based Tire Slip Controller," *Journal of Vehicle System Dynamics*, vol. 41, no. 6, pp. 477–511, 2004.

[4] K. Buckholtz, "Reference input wheel slip tracking using sliding mode control," in *SAE Technical Paper 2002-01-0301*, 2002.

[5] M. Tanelli, G. Osorio, M. di Bernardo, S. Savaresi, and A. Astolfi, "Limit Cycles Analysis in Hybrid Anti-lock Braking Systems." in *Proceedings of the 46th IEEE Conference on Decision and Control*, New Orleans, LA, 2007.

[6] T. Wakabayashi, T. Matsuto, K. Tani, and A. Ohta, "Development of Motor-actuated Antilock Brake System for Light Weight Motorcycle," *JSAE Review*, vol. 19, no. 4.

[7] R. J. Miennert, "Antilock Brake System Application to a Motorcycle Front Wheel," *SAE Preprints*, vol. n 740630, 1974.

[8] T. Hikichi, T. Tomari, M. Katoh, and M. Thiem, "Research on Motorcycle Antilock Brake System: part 2, Influence on Motorcycle Braking in Turn," in *Proceedings of the 23rd International Symposium on Automotive Technology and Automation*, Vienna, Austria, 1990.

[9] G. Ferretti, S. M. Savaresi, F. Schiavo, and M. Tanelli, "Modelling and simulation of motorcycle dynamics for Active Control Systems Prototyping," in *Proceedings of the 5th MATHMOD Conference, Vienna, Austria*, 2006.

[10] R. S. Sharp, "The stability and control of motorcycles," *Journal of Mechanical Engineering Science*, vol. 13, pp. 316–329, 1971.

[11] V. Cossalter and R. Lot, "A motorcycle multi-body model for real time simulations based on the natural coordinates approach," *Vehicle System Dynamics: International Journal of Vehicle Mechanics and Mobility*, vol. 37, pp. 423–447, 2002.

[12] H. B. Pacejka, *Tyre and Vehicle Dynamics*. Oxford: Buttherworth Heinemann, 2002.

[13] R. Lot, "A Motorcycle Tire Model for Dynamic Simulations: Theoretical and Experimental Aspects," *Meccanica*, vol. 39, pp. 207–220, 2004.

[14] R. S. Sharp, S. Evangelou, and D. J. N. Limebeer, "Advances in the modelling of motorcycle dynamics," *Multibody System Dynamics*, vol. 12, pp. 251–283, 2004.

[15] M. Corno, S. Savaresi, M. Tanelli, and L. Fabbri, "On Optimal Motorcycle Braking." *Control Engineering Practice*, vol. In Press.

[16] H. B. and B. R., "Brake-by-wire without mechanical backut using a ttp Communication Network," in *SAE Int. Cong. Exhibition*, Detroit, MI, 1998.

[17] G. Becker, "Quadratic Stability and Performanc of Linear Parameter-Dependend Systems," Ph.D. dissertation, Mechanical Engineering, University of California, Berkeley, 1993.

[18] F. Wu, "Control of linear parameter varying systems," Ph.D. dissertation, Mechanical Engineering, University of California, Berkeley, 1995.

[19] G. Becker and A. Packard, "Robust Performance of Linear Parametrically Varying Systems using Parametrically Dependent Linear Dynamic Feedback," *Systems and Control Letters*, vol. 23, pp. 205–215, 1994.

[20] G. J. Balas, "Linear, Parameter-Varying Control and its Application to a Turbofan Engine," *International Journal of Robust and Nonlinear Control*, vol. 12, pp. 763–796, 2002.